INTERACTION ·NOTES

Note 362

May 1979

A Study of the EMP Interaction with
Aircraft Over an Imperfect Ground Plane

C. Taylor
V. Naik
T. Crow

Mississippi State University
Mississippi State, MS 38762

Abstract

The study of thin wire configurations, in particular the isolated
single wire and crossed wires, above the ground plane has been conducted
utilizing analytical techniques primarily. The formulation is based on
transmission line theory and the singularity expansion method (SEM).
Natural frequencies, natural current modes and coupling coefficients
are determined. These results are compared with the results obtained
by earlier investigators using conventional numerical techniques.

INTERACTION ·NOTES

Note 362

May 1979

A Study of the EMP Interaction with
Aircraft Over an Imperfect Ground Plane

C. Taylor
V. Naik
T. Crow

Mississippi State University
Mississippi State, MS 38762

Abstract

The study of thin wire configurations, in particular the isolated
single wire and crossed wires, above the ground plane has been conducted
utilizing analytical techniques primarily. The formulation is based on
transmission line theory and the singularity expansion method (SEM).
Natural frequencies, natural current modes and coupling coefficients
are determined. These results are compared with the results obtained
by earlier investigators using conventional numerical techniques.

TABLE OF CONTENTS

LIST OF FIGURES

4

LIST OF TABLES

SECTION I

INTRODUCTION

A problem of continuing and widespread interest in electro-
magnetic theory is that of wire configurations under certain speci-
fic conditions. The transient and harmonic analyses of thin-wire
structures have been the subject of investigations for a number of
years. An early treatment of thin wires was given by Oseen [1] who
applied the method of retarded potentials to straight thin wires and
calculated the induced current on a wire by a transient incident
wave. Hallen [2] used a slightly different form and derived a pure
integral equation for the induced current on a thin wire and used it
to derive analytical expression for the natural frequencies and
current distributions of the natural modes. Since then many investi-
gations have studied various thin-wire problems.

In recent times Tesche [3] analyzed the thin wire scatterer
from the singularity expansion point of view. Wilton and Umashanker
[4] conducted a parametric study of an L shaped wire using the sing-
ularity expansion method (SEM). The EMP[*] interaction with a thin
wire above a ground plane using SEM was investigated numerically by
Shumpert [5]. However, in more recent times Crow, et al. [6] have
conducted an in depth study of the crossed wire structure using SEM.

Even though many of these papers are helpful in the determina-
tion of induced currents and charge densities on thin wire config-
urations, most of them utilize very complex and elaborate numerical

---

[*]The electromagnetic pulse generated by a nuclear denotation is
generally referred to as the EMP.

6

techniques. Being motivated by some techniques used earlier, the present investigation utilizes primarily analytical techniques for the treatment of wire configurations in the proximity of a lossy ground.

The second chapter of this report presents the time harmonic analysis and considers the plane wave illumination of a single wire over a perfect ground. The approach used follows Taylor, et al. [7] for the current distribution induced on a transmission line by a nonuniform field. Subsequently the plane wave illumination of crossed wire configuration over perfect ground is considered. The single wire and crossed wire configurations are then considered to be in the proximity of a lossy ground plane. The third chapter includes transient analysis with brief description of SEM. It presents the technique for determining the natural modes and frequencies for perfect ground, as well as lossy ground considerations utilizing SEM. Numerical results obtained for both single wire and crossed wire configuration are presented in Chapter IV. Chapter V contains the conclusions and comments.

The accurate determination of the natural frequencies and natural current modes on a mathematically tractable configuration (e.g., the crossed wire configuration) is an early step in the study of electromagnetic field interaction with an aircraft that will proceed to more complex configurations. This and other topics are considered in some detail in this report.

SECTION II

TIME HARMONIC ANALYSIS

2.1 Plane Wave Illumination of the Single Wire

Over Perfect Ground

Some time ago, Bates and Hawley [8] presented a simple first-
order treatment of the scattering of plane waves from an infinitely
thin wire above a ground plane. In that paper the effects due to a
lossy ground plane are neglected but they were later considered by
Leonard Schlessinger [9]. In more recent times Crow, et al. [6] and
[10], have also conducted similar studies for thin wires of finite
length above a perfect ground plane applying purely numerical tech-
niques.

The present investigation considers (utilizing simple analyti-
cal techniques) plane wave illumination of a single wire above a
ground plane. Initially, the perfect ground case is presented,
later the lossy ground plane case is discussed. In both cases
transmission line theory is used, which requires the wire height to
be much less than the wave length and the wire length.

In this section we obtain the expression for a single wire over
perfect ground illuminated by a plane wave. The general formulation
for the current distribution along the thin cylinder (or wire) due
to normal plane wave incidence has been obtained by Taylor, et al.
[7] for a two wire transmission line with arbitrary termination
impedances. For the problem considered here the single wire with
its electromagnetic images forms a two wire transmission line with

open ends, as shown in Figure 2.1. In Figure 2.2, the transmission line currents at the ends are zero (i.e., $I_o = I_\ell = 0$ because Z_o and Z_ℓ are infinite). Hence the expression becomes

$$I(z,j\omega) = \frac{-j}{Z_c \sin(k\ell)} [\sin k(z-\ell) \int_o^z K(u) \sin ku \, du$$

$$+ \sin(kz) \int_z^\ell K(u) \sin k(u-\ell) \, du] \qquad (2.1)$$

where

$$K(u) = [E_z^i(h,z) - E_z^i(-h,z)] = j \, 4 \, E_o \sin(kh)$$
$$k^2 = Y \, Z \quad ,$$

Y is the shunt admittance per unit length and Z the series impedance per unit length.

2.2 Plane Wave Illumination of a Crossed Wire Configuration Over a Perfect Ground

Several investigators have considered the plane wave illumination of wire configurations over perfect ground and in free space. Shumpert [5] has also analyzed thick wire configurations. Crow, et. al. [11], formulated the problem using Pocklington type integro-differential equations and studied it by means of the SEM. Numerical techniques were used to determine the natural frequencies and associated current modes. Analysis of crossed wires in a plane wave field was done by King [12]; however, recently Crow, et al. [5] utilized SEM techniques for perpendicular crossed wires over a perfectly conducting ground plane. In order to avoid the complicated numerical techniques, an attempt was made to obtain the natural

Ground Parameters: μ_o , ε_g , σ_g
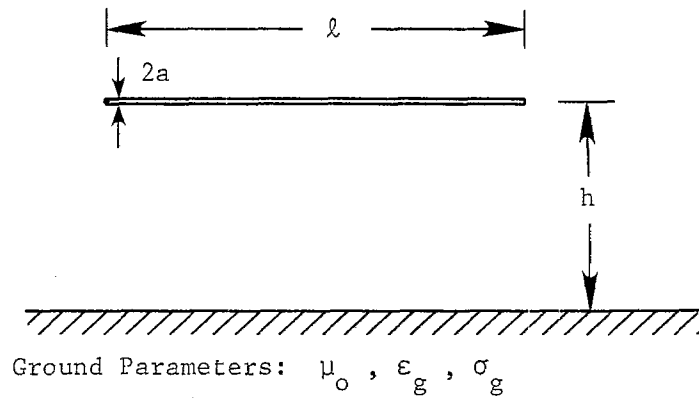
Figure 2.1: Thin wire above a lossy ground plane.
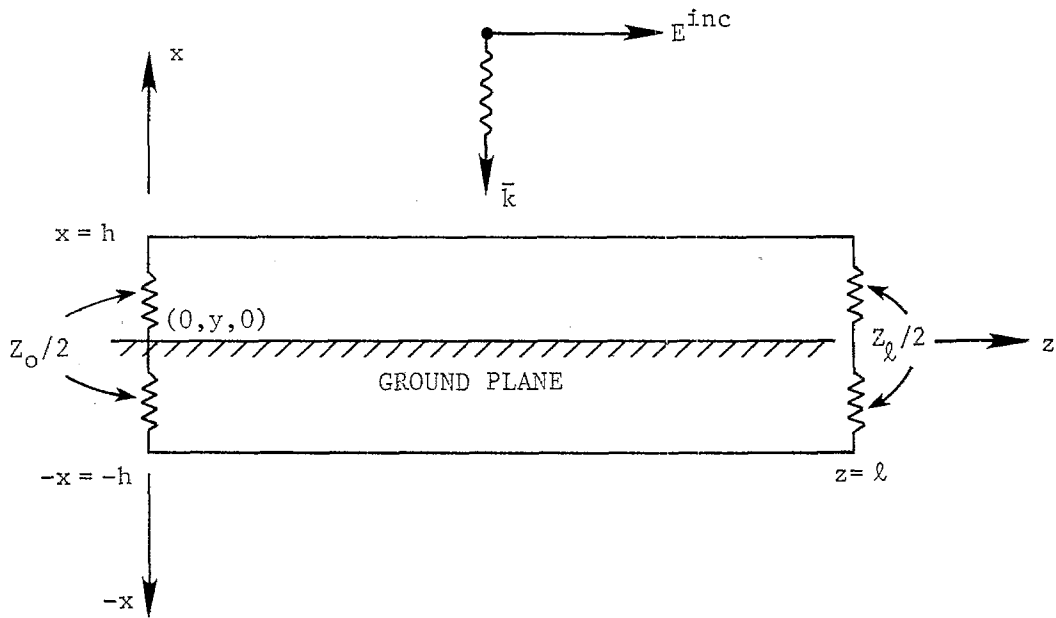
Figure 2.2: Terminated two-wire transmission line excited by a plane wave with normal incidence.

frequencies and associated current modes utilizing transmission line theory in conjunction with electromagnetic superposition.

Consider the wire configuration oriented as shown in Figure 2.3. Initially the current distributions are obtained considering excitation along the ℓ_a, ℓ_f or ℓ_ω elements separately. Then the net current distribution is obtained by the summation of the foregoing results via superposition.

Case A.   Consider the excitation along the ℓ_a element only. With reference to Figures 2.3 and 2.4 the current on the ℓ_a element is obtained by treating the configuration shown in Figure 2.3.

There are basically two junction conditions that apply to this configuration. (1) The Kirchhoff's current law must be satisfied at the crossed wire junction and (2) junction voltages of the wires are all equal. Hence Z_2 is infinite corresponding to the open end

$$\frac{1}{Z'_1} = \frac{2}{Z_\omega} + \frac{1}{Z_f} \tag{2.2}$$

and where Z_ω and Z_f are the impedances seen looking into the transmission line formed by the ℓ_ω and ℓ_f element with their images, from the junction, Z'_1 is the equivalent impedance formed considering Z_ω and Z_f impedances in parallel. Accordingly

$$Z_\omega = -j Z_{c\omega} \cot(k\ell_\omega) \tag{2.3}$$

where

$$Z_{c\omega} = 120 \ \ell n(2h/a_\omega) \tag{2.4}$$

and

$$Z_f = -j Z_{cf} \cot(k\ell_f) \tag{2.5}$$

11
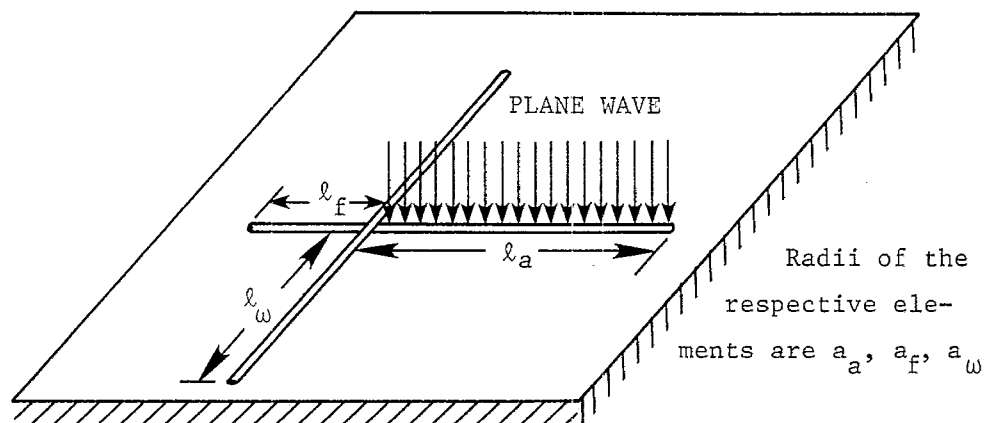
Figure 2.3:   Crossed wires oriented parallel to a ground
plane with the ℓ_a element excited by a plane
wave field.
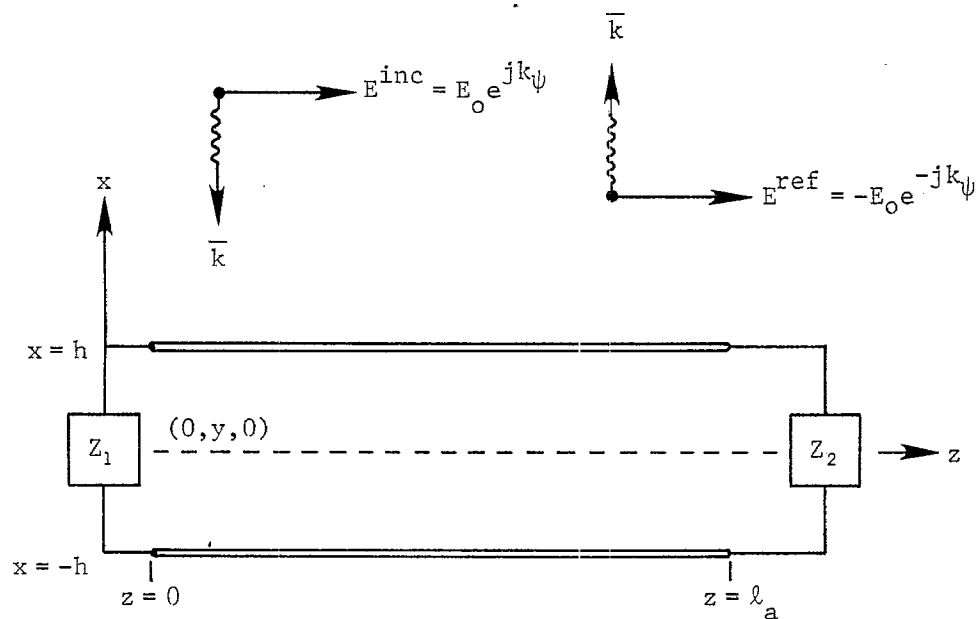
Figure 2.4:   Circuit diagram representing the configuration
shown in Figure 2.3, where Z_1 corresponds to the
junction impedence formed by ℓ_ω and ℓ_f elements.
Z_2 is infinite corresponding to the open end of
the ℓ_a element.

where

$$Z_{cf} = 120 \, \ell n(2h/a_f) \tag{2.6}$$

$Z_{c\omega}$ and Z_{cf} are the characteristic impedance of ℓ_ω and ℓ_f transmission lines respectively and correspond to the free space conditions.

According to Taylor, et al. [7], the current distribution induced on the line is

$$^*I_a'(z,j\omega) = I_2' \frac{\sin k\, z}{\sin k\, \ell_a} - I_1' \frac{\sin k(z-\ell_a)}{\sin k\, \ell_a} - \frac{j}{Z_{ca} \sin k\, \ell_a}$$

$$\cdot \left[\sin k\,(z-\ell_a) \int_0^z K(u) \cdot \sin k\, u \cdot du \right.$$

$$\left. + \sin k\, z \int_z^\ell K(u) \cdot \sin k(u-\ell_a) \cdot du \right] \tag{2.7}$$

Applying the free end conditions described earlier

$$I_2' = 0 \qquad \text{since} \quad Z_2 \quad \text{is infinite}$$

and

$$I_1' = \frac{-j}{Z_{ca} \cos k\, \ell_a + j\, Z_1 \sin k\, \ell_a} \int_0^{\ell_a} K(u) \cdot \sin k(u-\ell_a) \cdot du \tag{2.8}$$

Integrating and simplifying

$$K(z) = j\, 4\, E_o \, \sin k\, h \tag{2.9}$$

---

*Prime (') indicates the quantities when only the ℓ_a element is excited.

Using (2.8) and (2.9) in (2.7) yields

$$I'_a(z,j\omega) = -I'_1 \frac{\sin k(z-\ell_a)}{\sin k\ell_a} + \frac{4E_o \sin kh}{k\, Z_{ca} \sin k\ell_a} \cdot$$

$$\cdot [\sin k(z-\ell_a) + \sin k\ell_a - \sin kz] \qquad (2.10)$$

where

$$I'_1 = \frac{4E_o \sin kh}{k} \cdot \frac{(\cos k\ell_a) - 1}{Z_{ca} \cos k\ell_a + j Z_1 \sin k\ell_a} \qquad (2.11)$$

and

$$Z'_1 = -j \left[\frac{2\tan k\ell_\omega}{Z_{c\omega}} + \frac{\tan k\ell_f}{Z_{cf}} \right]^{-1} \qquad (2.12)$$

In order to obtain the current distribution on the other wire elements the junction voltage is used, i.e.,

$$V'_a(0,j\omega) = -I'_a(0,j\omega)Z'_1 = -I'_1 Z'_1 \qquad (2.13)$$

Now considering the ℓ_f element with its image an open ended transmission line the current distribution is

$$I'_f(z',j\omega) = I'_f(0,j\omega) \frac{\sin k(\ell_f - z')}{\sin k\ell_f} \qquad (2.14)$$

where a positive I_f current is directed away from the junction.*
The junction voltage then is

$$V'_f(0,j\omega) = + I'_f(0,j\omega)Z_f \qquad (2.15)$$

noting that

$$V'_f(0,j\omega) = V'_a(0,j\omega) \cdot$$

---

*The z' coordinate axis coincides with the z axis but is directed in the opposite direction.

14

Using (2.13) and (2.15) yields

$$I'_f(0,j\omega) = \frac{Z'_1}{Z_f} \frac{4E_o \sin k h}{k} \frac{(\cos k \ell_a) - 1}{Z_{ca} \cos k \ell_a + j Z'_1 \sin k \ell_a} \qquad (2.16)$$

Correspondingly for the ℓ_ω elements it can be shown that

$$I'_\omega(y,j\omega) = I'_\omega(0,j\omega) \frac{\sin k(\ell_\omega - y)}{\sin k \ell_\omega} \qquad .$$

where

$$I'_\omega(0,j\omega) = \frac{-Z_1}{Z_\omega} \frac{4E_o \sin k h}{k} \frac{(\cos k \ell_a) - 1}{Z_{ca} \cos k \ell_a + j Z'_1 \sin k \ell_a} \qquad (2.17)$$

with a positive current directed away from the junction.

Case B. Applying the same solution technique as utilized for Case A and considering the excitation along the ℓ_f element only, the current on ℓ_f is (for this case the incident field is directed in the $-z'$ direction requiring a corresponding sign change)

$$I''_f(z',j\omega) = -I''_1 \frac{\sin k(z' - \ell_f)}{\sin k \ell_f} \frac{4E_o \sin k h}{k Z_{cf} \sin k \ell_f}$$

$$\cdot \left[\sin k(z' - \ell_f) + \sin k \ell_f - \sin k z' \right] \qquad (2.18)$$

where

$$I''_1 = I''_f(0,j\omega) = - \frac{4E_o \sin k h}{k} \frac{(\cos k \ell_f) - 1}{Z_{cf} \cos k \ell_f + j Z''_1 \sin k \ell_f} \qquad . \qquad (2.19)$$

$$Z''_1 = -j \left[\frac{2 \tan k \ell_\omega}{Z_{c\omega}} + \frac{\tan k \ell_a}{Z_{ca}} \right]^{-1}$$

15

Due to the different coordinate axes being in opposite directions for ℓ_a and ℓ_f elements, there is sign difference between (2.18) and (2.19) and their corresponding equations, (2.10) and (2.11).

The current induced on ℓ_a element is

$$I_a''(z,j\omega) = I_a''(0,j\omega) \; \frac{\sin k (\ell_a - z)}{\sin k \ell_a} \tag{2.20}$$

where

$$I_a''(0,j\omega) = + \frac{Z_1''}{Z_a} \; \frac{4E_o \sin k \; h}{k} \; \frac{(\cos k \, \ell_f)-1}{Z_{cf}\cos k \, \ell_f + j \, Z_1'' \, \sin k \, \ell_f} \tag{2.21}$$

and the current induced on ℓ_ω element is

$$I_\omega''(y,j\omega) = I_\omega''(0,j\omega) \; \frac{\sin k (\ell_\omega - y)}{\sin k \, \ell_\omega} \; . \tag{2.22}$$

where

$$I_\omega''(0,j\omega) = + \frac{Z_1''}{Z_\omega} \; \frac{4E_o \sin k \; h}{k} \; \frac{(\cos k \, \ell_f)-1}{Z_{cf}\cos k \, \ell_f + j \, Z_1'' \; \sin k \, \ell_f} \; . \tag{2.23}$$

Case C. Once the current distribution over different elements is obtained due to excitation along ℓ_a and ℓ_f elements the total currents can be easily determined utilizing superposition theorem. It should be noted that the current distribution due to the plane wave excitation along the ℓ_ω elements can be inferred from the foregoing by using symmetry. To obtain the total currents for the entire structure, results for Case A are added to the corresponding results for Case B to yield,

16

$$I_\omega(z,j\omega) = I_\omega(0,j\omega) \frac{\sin k(\ell_\omega - z)}{\sin k \ell_\omega} \quad . \tag{2.24}$$

where

$$I_\omega(0,j\omega) = \frac{j 4 E_o \sin k h \left[-Z_f \tan\left(\frac{k\ell_a}{2}\right) + Z_a \tan\left(\frac{k\ell_f}{2}\right) \right]}{k[(Z_a + Z_f)Z_\omega + 2Z_a Z_f]} \tag{2.25}$$

Similarly for the ℓ_f element

$$I_f(z',j\omega) = I_f(0,j\omega) \frac{\sin k(\ell_f - z')}{\sin k \ell_f}$$

$$- \frac{4 E_o \sin k h}{k Z_{cf} \sin k \ell_f} [\sin k(z' - \ell_f) + \sin k \ell_f - \sin k z'] \tag{2.26}$$

where

$$I_f(0,j\omega) = \frac{-j 4 E_o \sin k h \left[(Z_\omega + 2Z_a) \tan\left(\frac{k\ell_f}{2}\right) + Z_\omega \tan\left(\frac{k\ell_a}{2}\right) \right]}{k[(Z_a + Z_f) Z_\omega + 2 Z_a Z_f]} \tag{2.27}$$

Lastly for the ℓ_a element

$$I_a(z,j\omega) = I_a(0,j\omega) \frac{\sin k(\ell_a - z)}{\sin k \ell_a}$$

$$+ \frac{4 E_o \sin k h}{k Z_{ca} \sin k \ell_a} [\sin k(z - \ell_a) + \sin k \ell_a - \sin k z] \tag{2.28}$$

where

$$I_a(0,j\omega) = \frac{j 4 E_o \sin k h \left[(Z_\omega + 2 Z_f) \tan\left(\frac{k \ell_f}{2}\right) + Z_\omega \tan\left(\frac{k\ell_a}{2}\right) \right]}{k[(Z_a + Z_f) Z_\omega + 2 Z_a Z_f]} \tag{2.29}$$

Note that the junction currents given by (2.25), (2.27) and (2.29) satisfy Kirchhoff's current law at the crossed wire junction.

2.3 Current Source Excitation of Crossed Wires Over a Perfect Ground Plane

To obtain all the natural current modes and frequencies it is convenient to consider the crossed wire structure to be driven from a current source as shown in Figures 2.5 and 2.6. Then applying transmission line theory, the current and voltage along the ℓ_ω element are

$$V_\omega(y, j\omega) = V_1 e^{-jky} + V_2 e^{jky} \quad . \tag{2.30}$$

$$I_\omega(y, j\omega) = \frac{1}{Z_{c\omega}} [V_1 e^{-jky} - V_2 e^{jky}] \quad . \tag{2.31}$$

where the following end conditions must be satisfied:

$$I_\omega(\ell_\omega, j\omega) = \frac{1}{Z_{c\omega}} [V_1 e^{-jk\ell_\omega} - V_2 e^{-jk\ell_\omega}] = I_o \tag{2.32}$$

and

$$\frac{V_\omega(0, j\omega)}{I_\omega(0, j\omega)} = -Z_T = Z_{c\omega} \frac{V_1 + V_2}{V_1 - V_2} = - \left[\frac{1}{Z_a} + \frac{1}{Z_f} + \frac{1}{Z_\omega} \right]^{-1} \quad . \tag{2.33}$$

On performing mathematical manipulation, (2.32) and (2.33) yield

$$V_1 = -j \frac{1}{2} \frac{Z_{c\omega}(Z_{c\omega} - Z_T)}{Z_\omega + Z_T} \frac{I_o}{\mathrm{Sin}\, k\, \ell_\omega} \tag{2.34}$$

$$V_2 = +j \frac{1}{2} \frac{Z_{c\omega}(Z_{c\omega} + Z_T)}{Z_\omega + Z_T} \frac{I_o}{\mathrm{Sin}\, k\, \ell_\omega} \tag{2.35}$$

Using (2.34) and (2.35) in (2.31) yields

$$I_\omega(y, j\omega) = I_o' [Z_{c\omega}(e^{-jky} + e^{jky}) - Z_T(e^{-jky} - e^{jky})] \tag{2.36}$$
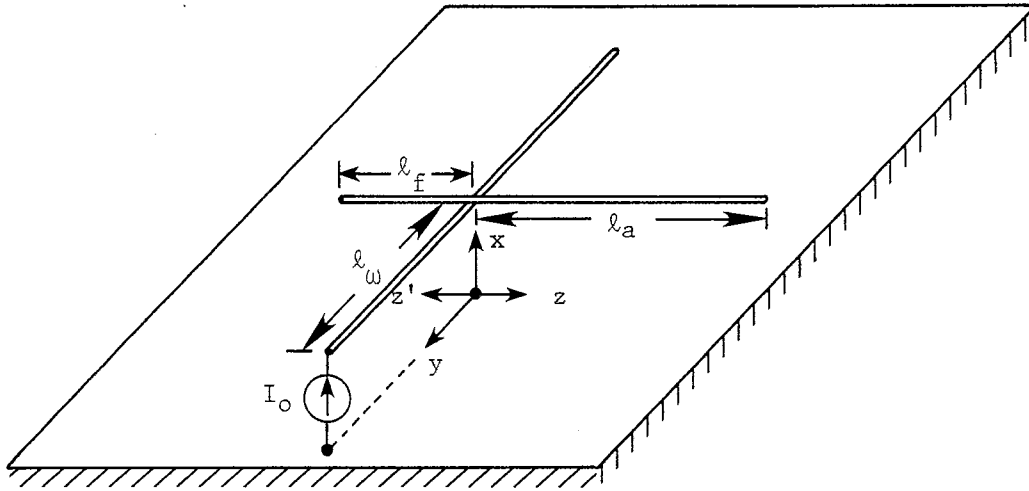
Figure 2.5:   Current source excitation of the crossed wire
configuration over a perfect ground.
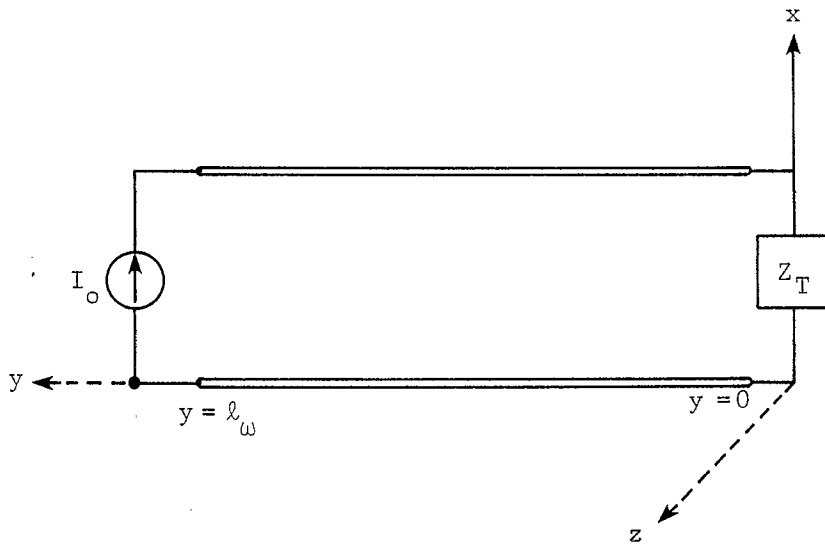
Figure 2.6:   Transmission line equivalent circuit for the
configuration shown in Figure 2.5.

where

$$I_o' = -j \frac{I_o}{2(Z_\omega + Z_T)\sin k\ell_\omega} \tag{2.37}$$

Therefore

$$I_\omega(y,j\omega) = j \frac{Z_{c\omega}\cos k y + j Z_T \sin k y}{(Z_\omega + Z_T)\sin k\ell_\omega} I_o \tag{2.38}$$

or

$$I_\omega(y,j\omega) = \frac{Z_{c\omega}\cos k y + j Z_T \sin k y}{Z_{c\omega}\cos k\ell_\omega + j Z_T \sin k\ell_\omega} I_o \tag{2.39}$$

where

$$Z_T = \frac{Z_a Z_f Z_\omega}{Z_f Z_\omega + Z_a Z_\omega + Z_a Z_f} \tag{2.40}$$

and is the parallel combination of all elements except the one that is excited. The current on the ℓ_ω element that is not excited and on the ℓ_a and ℓ_f elements may be obtained by the use of Kirchhoff's current law at the junction,

$$-I_\omega(0,j\omega) = I_a(0,j\omega) + I_\omega'(0,j\omega) + I_f(0,j\omega) \tag{2.41}$$

and the junction voltage conditions,

$$V_\omega(0,j\omega) = -I_a(0,j\omega)Z_a = -I_f(0,j\omega)Z_f = -I_\omega'(0,j\omega)Z_\omega \tag{2.42}$$

Hence the current on the ℓ_ω element that is not driven is

$$\left(1 + \frac{Z_\omega}{Z_a} + \frac{Z_\omega}{Z_f}\right) I_\omega'(0,j\omega) = -I_\omega(0,j\omega) \quad . \tag{2.43}$$

The currents on other elements of the wire configuration can be obtained similarly. They are*

$$I'_\omega(y',j\omega) = I'_\omega(0,j\omega) \frac{\sin k(\ell_\omega - y')}{\sin k \ell_\omega} \tag{2.44}$$

$$I_a(z,j\omega) = I_a(0,j\omega) \frac{\sin k(\ell_a - z)}{\sin k \ell_a} \tag{2.45}$$

$$I_f(z',j\omega) = I_f(0,j\omega) \frac{\sin k(\ell_f - z')}{\sin k \ell_f} \tag{2.46}$$

where from (2.43) and (2.39)

$$I'_\omega(0,j\omega) = +j \frac{Z_T Z_{c\omega}}{Z_\omega(Z_\omega + Z_T)} \frac{I_o}{\sin k \ell_\omega} \cdot \tag{2.47}$$

Correspondingly for the ℓ_a and ℓ_f elements,

$$I_a(0,j) = +j \frac{Z_T Z_{c\omega}}{Z_a(Z_\omega + Z_T)} \frac{I_o}{\sin k \ell_\omega} \tag{2.48}$$

$$I_f(0,j\omega) = +j \frac{Z_T Z_{c\omega}}{Z_f(Z_\omega + Z_T)} \frac{I_o}{\sin k \ell_\omega} \tag{2.49}$$

When the ℓ_a element is excited by a current source, the current on ℓ_a, ℓ_f and ℓ_ω elements can be derived in a similar manner and are presented as follows

---

*Note that the y' axis coincides with the y axis except that it is directed in the opposite direction

$$I_a(z,j\omega) = -u \; \frac{Z_{ca} \cos k \, z + j \, Z_1' \sin k \, z}{(Z_a + Z_1') \sin k \, \ell_a} \; I_o \quad\quad (2.50)$$

$$I_\omega'(y',j\omega) = I_\omega'(0,j\omega) \; \frac{\sin k(\ell_\omega - y')}{\sin k \, \ell_\omega} \quad\quad (2.51)$$

$$I_\omega(y,j\omega) = I_\omega(0,j\omega) \; \frac{\sin k(\ell_\omega - y)}{\sin k \, \ell_\omega} \quad\quad (2.52)$$

$$I_f(z',j\omega) = I_f(0,j\omega) \; \frac{\sin k(\ell_f - z')}{\sin k \, \ell_f} \qu\quad (2.53)$$

where

$$I_\omega'(0,j\omega) = + j \; \frac{Z_1' \, Z_{ca} \, I_o}{Z_\omega'(Z_a + Z_1') \sin k \, \ell_a} \qu\quad (2.54)$$

$$I_\omega(0,j\omega) = + j \; \frac{Z_1' \, Z_{ca} \, I_o}{Z_\omega(Z_a + Z_1') \sin k \, \ell_a} \qu\quad (2.55)$$

$$I_f(0,j\omega) = + j \; \frac{Z_1' \, Z_{ca} \, I_o}{Z_f(Z_a + Z_1') \sin k \, \ell_a} \qu\quad (2.56)$$

and Z_1' has been defined previously.

Similarly when the ℓ_f element is excited the currents on ℓ_a, ℓ_f and ℓ_ω elements are

$$I_f(z',j\omega) = -j \; \frac{Z_{cf} \cos k \, z' + j \, Z_1'' \sin k \, z'}{(Z_f + Z_1'') \sin k \, \ell_f} \; I_o \qu\quad (2.57)$$

$$I_\omega'(y',j\omega) = I_\omega'(0,j\omega) \; \frac{\sin k(\ell_\omega - y')}{\sin k \, \ell_\omega} \qu\quad (2.58)$$

22

$$I_\omega(y,j\omega) = I_\omega(0,j\omega) \, \frac{\sin k(\ell_\omega - y)}{\sin k \, \ell_\omega} \qquad (2.59)$$

$$I_a(z,j\omega) = I_a(0,j\omega) \, \frac{\sin k(\ell_a - z)}{\sin k \, \ell_a} \qquad (2.60)$$

where

$$I_\omega'(0,j\omega) = +j \, \frac{Z_1'' \, Z_{cf} \cdot I_o}{Z_\omega'(Z_f + Z_1'') \sin k \, \ell_f} \qquad (2.61)$$

$$I_\omega(0,j\omega) = +j \, \frac{Z_1'' \, Z_{cf} \cdot I_o}{Z_\omega(Z_f + Z_1'') \sin k \, \ell_f} \qquad (2.62)$$

$$I_a(0,j\omega) = +j \, \frac{Z_1'' \, Z_{cf} \cdot I_o}{Z_a(Z_f + Z_1'') \sin k \, \ell_f} \qquad (2.63)$$

and Z_1'' has been defined previously.

2.4 Lossy Ground Plane Considerations

The propagation constant encountered in the earlier sections is a real quantity for the perfect ground case only. However, under lossy ground conditions the propagation constant becomes complex. Although only a few investigators have considered the treatment of wires over a lossy ground plane, there has been remarkable progress. Schlessinger [9] derived a self contained expression for the propagation constant following Sunde [13] and Wait [14].

Sunde [13] derived the propagation constant for insulated aerial conductors, accounting the finite conductivity of the earth which gives rise to an increase in the longitudinal impedance and to

23

resistance losses in the earth. He derived this expression as a special case of wire of infinite length above the surface of the earth.

According to Sunde the series distributed inductance can be approximated "with satisfactory accuracy for engineering purposes" as

$$L = \frac{\mu}{2\pi} \ln \frac{2(1 + \gamma_g h)}{\gamma_g a} \tag{2.64}$$

where

$$\gamma_g = \sqrt{j\omega\mu (\sigma_g + j\omega\varepsilon_g)} \tag{2.65}$$

with σ_g and ε_g the ground conductivity and permittivity, respectively. The shunt distributed capacitance is approximated by

$$C = \frac{2\pi\varepsilon_o}{\ln(\frac{2h}{a})} \tag{2.66}$$

According to the foregoing the product of the distributed series impedance and shunt admittance is

$$ZY \simeq \frac{(j\omega)^2 \varepsilon_o \mu_o}{\ln(\frac{2h}{a})} \left[\ln \left(\frac{1+\gamma_g g}{\gamma_g h} \right) + \ln \left(\frac{2h}{a} \right) \right] \tag{2.67}$$

Since the propagation constant $k = -j\sqrt{YZ}$, then

$$k \simeq -j \gamma_o \left[1 + \frac{1}{\ln\left(\frac{2h}{a}\right)} \cdot \ln \left(\frac{1 + \gamma_g h}{\gamma_g h} \right) \right]^{\frac{1}{2}} \tag{2.68}$$

where $\gamma_o = j\omega\sqrt{\mu_o \varepsilon_o}$.

All the foregoing expressions for the current induced on the

wire configurations over a ground plane became valid for the lossy

ground when the propagation constant of (2.68) is used in the

transmission line current and voltage expressions.

SECTION III

TRANSIENT ANALYSIS

3.1 Singularity Expansion Method

The SEM technique was recently introduced by Baum [15] as a
technique for efficiently characterizing a conducting bodies'
response to either transient or steady state electromagnetic illum-
ination. An arbitrarily shaped conducting object is completely
characterized by its complex natural frequencies together with its
associated natural current mode distributions. The method may be
viewed as an extension of ordinary circuit theory methods to distrib-
uted parameter systems. Many of the recent EMP interaction investi-
gations and studies have utilized the SEM technique. Because of its
advantages the SEM technique is applied to the wire configurations
that are considered in the foregoing.

Initially a 3 x 1 vector is formed whose elements are the
current distributions on the crossed wires, i.e.,

$$\tilde{\vec{I}}(\vec{r},s) = \begin{bmatrix} I_f(z',s) \\ I_a(z,s) \\ I_\omega(y,s) \end{bmatrix}$$

where $s = j\omega$ and is the complex frequency, the tilde (~) denotes
the Laplace transform.

Then utilizing singularity expansion technique, the solution
for the wire currents may be expressed as

$$\tilde{\vec{I}}(\vec{r},s) = E_o \sum_{\alpha=1}^{\infty} \frac{\eta_\alpha}{s - s_\alpha} \vec{i}_\alpha(\vec{r}) \quad . \tag{3.1}$$

η_α is the coupling coefficient and $\vec{i}_\alpha(\vec{r})$ is the αth natural mode and where the natural frequencies s_α are those nontrivial complex frequencies obtained by the complex values of s that yield

$$I_f^{-1}(z',s) = 0 \tag{3.2}$$

or

$$I_f^{-1}(z,s) = 0 \tag{3.3}$$

or

$$I_\omega^{-1}(y,s) = 0 \tag{3.4}$$

The vector $\vec{i}_\alpha(\vec{r})$ represents the normalized current distribution for the αth natural frequency or the αth natural current mode. It is defined as

$$\vec{i}_\alpha(\vec{r}) = \lim_{s \to s_\alpha} \frac{s - s_\alpha}{c_1 E_o} \tilde{\vec{I}}(\vec{r},s) \quad . \tag{3.5}$$

where c_1 is a constant adjusted so that the maximum value of any element of $i_\alpha(r)$ is equal to 1.

Accordingly then the coupling coefficient η_α is defined such that

$$\eta_\alpha \vec{i}_\alpha(\vec{r}) = \lim_{s \to s_\alpha} \frac{s - s_\alpha}{E_o} \tilde{\vec{I}}(\vec{r},s) \tag{3.6}$$

However, it should be noted that the natural frequencies (or simple pole singularities) of $\vec{I}(\vec{r},s)$ occur in complex conjugate pairs since

27

the current must be purely real in the time domain. If only the frequencies of the third quadrant of the complex s-plane are considered then the time domain solution for impulse excitation is

$$\vec{I}(\vec{r},t) = 2 E_o \sum_{\alpha=1}^{\infty} Re \left[\eta_\alpha \ e^{s_\alpha t} \ \vec{i}_\alpha(\vec{r}) \right] . \qquad (3.7)$$

3.2 Natural Frequencies and Associated Natural Current Modes for a Perfect Ground

Plane wave illumination of the single wire over perfect ground has been formulated in section 2.1. In this section we obtain the natural frequencies for this configuration and compare the results with those obtained by other investigators utilizing different approaches.

From equation (2.1)

$$I(z,j\omega) = \frac{4 \ E_o \ \sin k \ h}{k \ Z \ \sin k \ \ell} \ [\sin k(z - \ell) + \sin k \ \ell - \sin k \ z] \qquad (3.8)$$

in which all parameters have been defined earlier. Note that the current $I(z,j\omega)$ diverges at natural frequencies for which

$$\sin k \ \ell = 0 \qquad (3.9)$$

or when

$$k = \frac{n\pi}{\ell} . \qquad (3.10)$$

n = 1, 2, 3, ... where ℓ is the wire length.

For the perfect ground case and free space conditions above the ground the propagation constant is purely real

$$k = -j \sqrt{YZ} = \omega\sqrt{LC} \tag{3.11}$$

where the characteristic impedance of the transmission line formed by the single wire and its image is

$$Z_c = \sqrt{\frac{L}{C}} \tag{3.12}$$

Thus

$$\omega = \frac{1}{\sqrt{\mu\varepsilon}} \frac{n\pi}{\ell} \tag{3.13}$$

relates the natural frequencies that are observed to be independent of the height above the ground. These natural frequencies being purely real differ from the complex ones found by Tesche [3] for the wires in free space, (a different physical configuration), but are similar to the ones determined by Umashanker, Shumpert and Wilton [16] for wires over a perfect ground plane.

The crossed wire configuration is more difficult to analyze in that there are two independent conditions for which the induced currents diverge and one requires a numerical search for the natural frequencies. Both divergence conditions occur for the current source excitation (section 2.3) but only one condition arises when plane wave excitation is considered (section 2.2).

In the first attempt to obtain the frequencies for which the currents in (2.42), (2.50), (2.51) and (2.52) may diverge, it is

noted that both (2.42) and (2.50) diverge as $Z_\omega \to 0$ since

$$Z_T \xrightarrow[Z_\omega \to 0]{} Z_\omega$$

and

$$I'_\omega(0,j\omega) \xrightarrow[Z_\omega \to 0]{} j \ \frac{Z_{c\omega} \ I_o}{2 \ \sin \ k \ \ell_\omega} \ \frac{1}{Z_\omega} \qquad (3.14)$$

where

$$Z_\omega \ = \ -j \ Z_{c\omega} \ \frac{\cos \ k \ \ell_\omega}{\sin \ k \ \ell_\omega}$$

Accordingly the natural frequencies are the frequencies for which $Z_\omega = 0$. Hence they satisfy

$$k\ell_\omega \ = \ (2\alpha - 1) \ \frac{\pi}{2} \qquad = 1, \ 2, \ 3, \ \ldots$$

Or in the complex s-plane the natural frequencies are

$$s_\alpha \ = \ j(2\alpha - 1) \ \frac{\pi}{2\ell_\omega} \qquad \alpha \ = 1, \ 2, \ 3, \ \ldots$$

However, it should be noted that I_a and I_f remain finite at the foregoing natural frequencies.

A second condition for which the crossed wire currents diverge is

$$Z_\omega + Z_T \ = \ 0$$

The frequencies for which the foregoing is satisfied can be obtained by a numerical search routine programmed for the digital computer.

30

The natural current modes are then determined for the associated natural frequencies as follows; e.g., considering the first natural frequency $k_1 \ell_\omega = 2.568$. By trial and error it is found that I_a is larger than I_f and I_ω at $k = k_1$. For this frequency I_o is then adjusted so that

$$I_a(z, j\omega_1) = \frac{\sin k_1(\ell_a - z)}{\sin k_1 \ell_a} \qquad (3.15)$$

$$I_f(z', j\omega_1) = -0.1506 \frac{\sin k_1(\ell_f - z')}{\sin k_1 \ell_f} \qquad (3.16)$$

$$I_{\omega_1}(y, j\omega) = -I_{\omega_1}(y', \omega) = -0.4291 \frac{\sin k_1(\ell_\omega - y')}{\sin k_1 \ell_\omega} \qquad (3.19)$$

Plots of the first six natural modes for crossed wires over a ground plane are shown in Figures 4.1 through Figure 4.6. Analytic results are also presented in Appendix A.

3.3 Natural Frequencies for a Lossy Ground Plane

The natural frequencies for wires over a lossy ground plane are obtained by using Chapter II and the divergence condition (3.10). Hence the natural frequencies for a single wire are obtained by finding the frequencies for which the following is satisfied

$$-j\gamma_o \left[1 + \frac{1}{\ell n\left(\frac{2h}{a}\right)} \cdot \ell n \left(\frac{1 + \gamma_g h}{\gamma_g h}\right)\right]^{\frac{1}{2}} = \frac{\alpha \pi}{\ell}$$

This expression must be solved numerically to obtain the natural frequency for each integer α. Results are presented in Chapter IV.

SECTION IV

NUMERICAL RESULTS

The numerical technique used to obtain the natural frequencies for single wire and crossed wires, essentially utilizes search routines which scan the area of interest in the complex s-plane. Thus, the natural frequencies which satisfy the expression in question are determined. The computer program utilized for the same is referenced by Crow, et al. [6]. It uses a subroutine which is based on the Cauchy integral formula and determines the zeros of the analytical function $F(z)$ for the induced current expressions. On obtaining the results, R expresses the ratio of the function $F(z)$ to the average magnitude of $F(z)$ evaluated at points along a selected search contour. It should be noted that an accurate zero of the function would be represented by values of $R \leq 0.1$

Tables 4.1 and 4.2 show the natural frequencies for a thin wire above a ground plane with typical conductivities and dielectric constants for concrete with $a = 0.5$ m, $h = 1.0$ m and $\ell = 10.0$ m (for Table 4.1) and $a = 2.0$ m, $h = 4.0$ m and $\ell = 40.0$ m for Table 4.2 respectively. In Tables 4.3 and 4.4 are presented natural frequencies for the thin wire above a ground plane for different heights with conductivity $\sigma_g = 0.0076$ and $\varepsilon_g' =$ dielectric constant $= 25.0$ for $a = 0.5$ m and $\ell = 10.0$ m. Table 4.3 is valid for $n = 1.0$ and Table 4.4 is valid for the $n = 2.0$ case. The natural frequencies for the crossed wire structure over a perfect ground

32

TABLE 4.1[*]   NATURAL FREQUENCIES FOR THIN WIRE ABOVE LOSSY GROUND
(a = 0.5 m, h = 1.0 m, ℓ = 10.0 m, α = 1 mode)

a = Radius of the wire = 0.5 m
h = Height of the wire above the ground = 1.0 m
ℓ = Length of the wire = 10.0 m

(S_α/c)		Ratio (R)	Ground (σ_g) Conductivity	Dielectric Constant (ε'_g)[**]
Real	Imaginary			
−0.05102414	0.27835674	0.1001 x 10^{-5}	0.0076 mho/m	25.0
−0.04831029	0.27238492	0.2563 x 10^{-6}	0.009 mho/m	20.0

TABLE 4.2[*]   NATURAL FREQUENCIES FOR THIN WIRE ABOVE LOSSY GROUND
(a = 2.0 m, h = 4.0 m, ℓ = 40.0 m, α = 1 mode

a = Radius of the wire = 2.0 m
h = Height of the wire above the ground = 4.0 m
ℓ = Length of the wire = 40.0 m

(S_α/c)		Ratio (R)	Ground (σ_g) Conductivity	Dielectric Constant (ε'_g)
Real	Imaginary			
−0.00877793	0.07124597	0.4858 x 10^{-6}	0.0066 mho/m	35.0
−0.00778715	0.07052281	0.1143 x 10^{-5}	0.0076 mho/m	25.0
−0.00692798	0.07059135	0.1270 x 10^{-5}	0.009 mho/m	20.0

[*]With reference to Figure 2.1

[**]$\varepsilon_g = \varepsilon'_g \cdot \varepsilon_o$ where ε'_g is called the dielectric constant, ratio (R) = $\dfrac{\text{magnitude of } F(Z)}{\text{average magnitude}}$

TABLE 4.3* NATURAL FREQUENCIES FOR THIN WIRE AT
DIFFERENT HEIGHTS ABOVE LOSSY GROUND
PLANE ($\alpha = 1$ mode)

a = radius of the wire = 0.5 m , ℓ = length of the wire = 10.0 m

σ_g = ground conductivity = 0.0076 mho/m, ε_g' = dielectric

constant = 25.0

$$(\varepsilon_g = \varepsilon_g' \varepsilon_o)$$

Height (h) above ground (m)	Ratio (R)	(S_α/c)	
		Real	Imaginary
1.0	0.1001×10^{-5}	-0.05102414	0.27835674
1.5	0.2331×10^{-5}	-0.03077844	0.29960148
2.0	0.5121×10^{-6}	-0.02093694	0.30609920
2.5	0.6837×10^{-6}	-0.01550837	0.30892346
3.0	0.1127×10^{-5}	-0.01215137	0.31041838
3.5	0.1656×10^{-6}	-0.00990076	0.31131393
4.0	0.3717×10^{-3}	-0.00830301	0.31190006
4.5	0.3627×10^{-6}	-0.00711283	0.31230273
5.0	0.2166×10^{-6}	-0.0061997	0.31259685
5.5	0.3973×10^{-6}	-0.0054785	0.31281843
6.0	0.4237×10^{-6}	-0.0048962	0.31299033
6.5	0.8557×10^{-7}	-0.0044173	0.31312691
7.0	0.2168×10^{-6}	-0.00401720	0.31323763
7.5	0.6561×10^{-6}	-0.00367852	0.31332891
8.0	0.6561×10^{-6}	-0.00338850	0.31340527
8.5	0.2344×10^{-6}	-0.00313765-	0.31346994
9.0	0.6883×10^{-6}	-0.00291877	0.31352531
9.5	0.6669×10^{-6}	-0.00272628	0.31357319
10.0	0.4135×10^{-7}	-0.00255806	0.31361494

* With reference to Figure 2.1.

TABLE 4.4[*]   NATURAL FREQUENCIES FOR THIN WIRE AT
              DIFFERENT HEIGHTS ABOVE LOSSY GROUND
              PLANE (α = 2 mode)

a = radius of the wire = 0.5 m, ℓ = length of the wire = 10.0 m

σ_g = ground conductivity = 0.0076 mho/m, ε'_g = dielectric
constant = 25.0

$$(\varepsilon_g = \varepsilon'_g \, \varepsilon)$$

Height (h) above ground (m)	Ratio (R)	(S_α/c) Real	Imaginary
1.2	0.1045×10^{-5}	−0.049947285	0.61470751
1.5	0.1923×10^{-5}	−0.03549272	0.62016536
2.0	0.1050×10^{-3}	−0.02321064	0.6238932
2.5	0.1050×10^{-4}	−0.01697165	0.6254712
3.0	0.9174×10^{-5}	−0.01307539	0.6262959
3.5	0.3516×10^{-6}	−0.01057798	0.6267861
4.0	0.2020×10^{-6}	−0.00882479	0.6271039
4.5	0.5290×10^{-6}	−0.00753400	0.6273233
5.0	0.2724×10^{-7}	−0.0065484	0.6274822
5.5	0.1744×10^{-6}	−0.00577389	0.6276017
6.0	0.1720×10^{-6}	−0.00515098	0.6276942
6.5	0.3420×10^{-6}	−0.00464030	0.6277676
7.0	0.1746×10^{-6}	−0.00421481	0.6278270
7.5	0.3388×10^{-6}	−0.00385542	0.6278759
8.0	0.1723×10^{-6}	−0.00354826	0.6279168
8.5	0.5032×10^{-6}	−0.00328301	0.6279514
9.0	0.3131×10^{-7}	−0.00305189	0.6279810
9.5	0.1687×10^{-6}	−0.00284889	0.6280066
10.0	0.1742×10^{-6}	−0.00266932	0.6280289

*With reference to Figure 2.1

plane are shown in Table 4.5 for $\ell_a + \ell_f = 1.0\ L$, $\ell_f/\ell_a = 0.5$ and $a = 0.05\ L$ (where L is a scale factor). The natural current modes for these frequencies (first through the sixth) are shown in Figure 4.1 through Figure 4.6. A comparison of these modes with the numerically obtained modes of Crow, et al. [6] exhibits very close agreement. Lastly, the natural frequencies as obtained by Crow, et al. [6] for the crossed wire configuration accounting the radiation losses (with the same dimensions as considered for results in Table 4.5) is shown in Table 4.6 for the purpose of comparison. It should be pointed out that radiation losses could be incorporated into the presented analysis using the procedure suggested by Marin [17]. This is reserved for future study.

Coupling coefficient calculations are presented in Appenix A which completes the SEM analysis for the crossed wires over a lossy ground plane.

TABLE 4.5*   NATURAL FREQUENCIES FOR CROSSED WIRE
CONFIGURATION OVER A GROUND PLANE FOR
$\ell_a + \ell_f = L$, $\ell_a/\ell_f = 1.9412$ (using current
source excitation).

α	S_α/Lc
1	j 2.5680
2	j 3.1416
3	j 4.0157
4	j 6.2834
5	j 7.9421
6	j 9.4248
7	j10.9614
8	j12.5665
9	j14 6468
10	j15.7080

*With reference to Figures 2.3 and 2.5

TABLE 4.6   NATURAL FREQUENCIES FOR CROSSED WIRES (as
obtained by Crow, et al.) FOR $\ell_a + \ell_f = L$,
$\ell_a/\ell_f = 2$; $h/L = 0.1$, $a/L = 0.05$.

α	$S_\alpha L/c$	
1	−0.0202	j 2.4525
2	−0.0426	j 2.7604
3	−0.0470	j 3.9166
4	−0.1775	j 5.9389
5	−0.3015	j 7.7876
6	−0.3289	j 8.3861
7	−0.5359	j10.7325
8	−0.8424	j12.0186
9	−0.7667	j14.1852

$$\alpha = 1$$

$$\frac{s_\alpha L}{c} = j2.57$$

Figure 4.1: Natural current mode for a crossed wire structure over a ground plane, transmission line formulation results for $L = 2\ell_\omega = \ell_a + \ell_f$, $\ell_a/\ell_f = 1.9412$ (arrows indicate directions assumed for positive current).
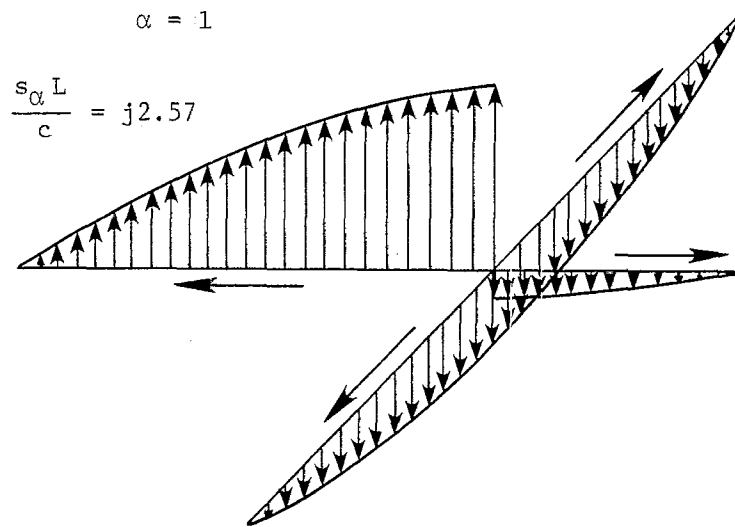
Figure 4.2: Natural current mode for a crossed wire
structure over a ground plane, trans-
mission line formulation results for
$L = 2\ell_\omega = \ell_a + \ell_f$, $\ell_a/\ell_f = 1.9412$ (arrows
indicate directions assumed for positive
current).

$$\alpha = 3$$

$$\frac{s_\alpha L}{c} = j \ 4.0157$$

Figure 4.3: Natural current mode for a crossed wire structure over a ground plane, transmission line formulation results for $L = 2\ell_\omega = \ell_a + \ell_f$, $\ell_a/\ell_f = 1.9412$ (arrows indicate directions assumed for positive current).
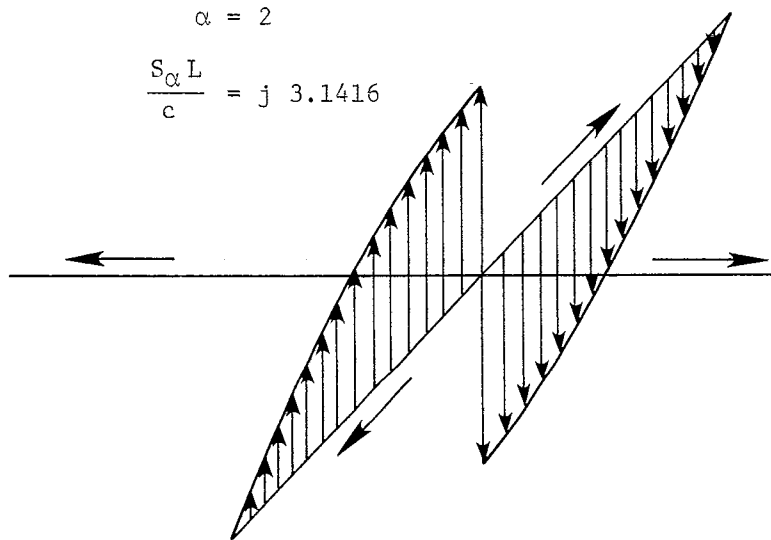
$$\alpha \;=\; 4$$

$$\frac{s_\alpha L}{c} \;=\; j\,6.28344$$

Figure 4.4: Natural current mode for a crossed wire
structure over a ground plane, trans-
mission line formulation results for
$L = 2\ell_\omega = \ell_a + \ell_f$, $\ell_a/\ell_f = 1.9412$ (arrows
indicate directions assumed for positive
current).
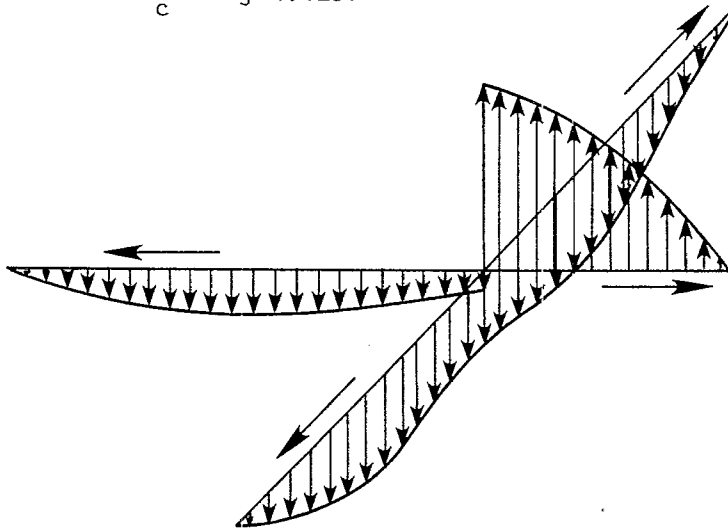
$$\alpha = 5$$

$$\frac{s_\alpha L}{c} = j\,7.9421$$

Figure 4.5: Natural current mode for a crossed wire structure over a ground plane, transmission line formulation results for $L = 2\ell_\omega = \ell_a + \ell_f$, $\ell_a/\ell_f = 1.9412$ (arrows indicate directions assumed for positive current).
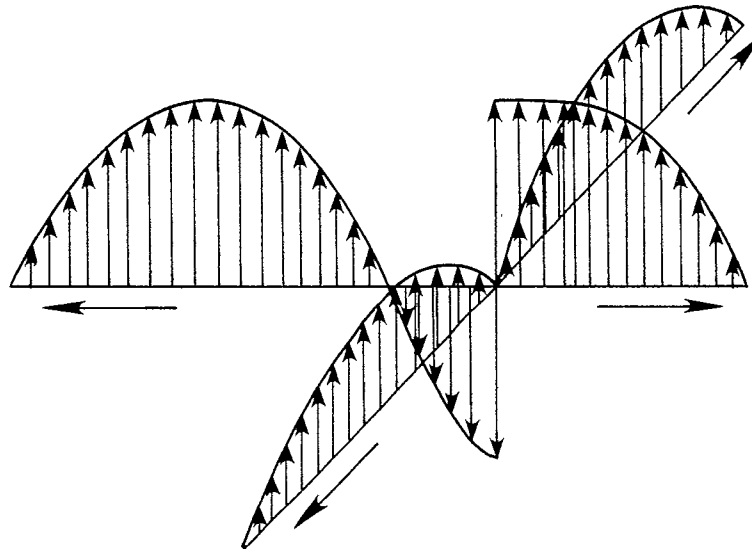
$$\alpha = 6$$

$$\frac{s_\alpha L}{c} = j\ 9.4248$$

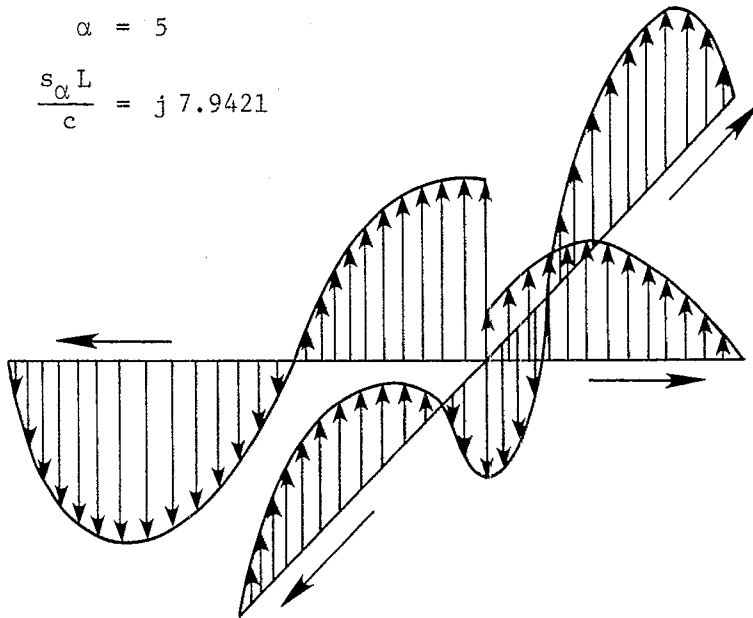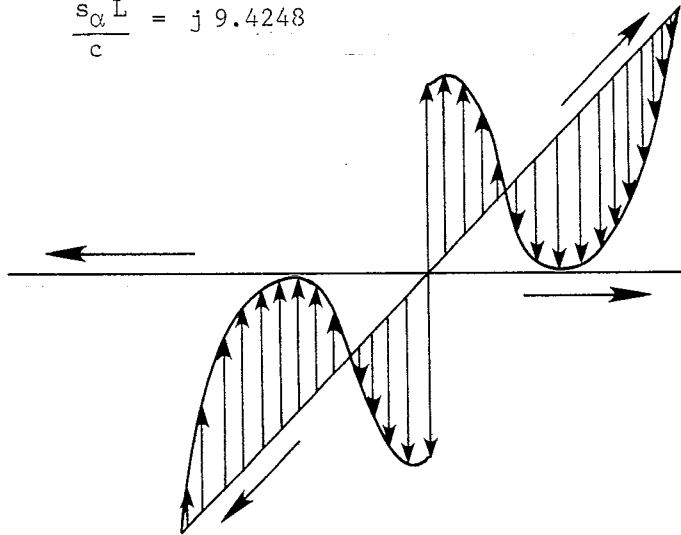
Figure 4.6: Natural current mode for a crossed wire structure over a ground plane, transmission line formulation results for $L = 2\ell_\omega = \ell_a + \ell_f$, $\ell_a/\ell_f = 1.9412$ (arrows indicate directions assumed for positive current).

SECTION V

CONCLUSION AND COMMENTS

The study of wire configurations in the proximity of lossy
ground is useful in the EMP simulation studies of aircraft [18].
As compared to other more elaborate, complex and purely numerical
techniques utilized for this interaction problem. the theoretical-
numerical approach presented here is much simpler. Besides, the
step-by-step approach enables the reader to obtain a clear under-
standing of the interaction problem.

In case of a single wire over a perfectly conducting ground
plane, the natural frequencies, as shown in section 3.2, are inde-
pendent of the height above the ground. It should also be noted
that in this case the imaginary parts of the natural frequencies
are close to those of the wire in free space. For the single wire
above lossy ground plane the natural frequencies for different
ground parameters are tabulated in Chapter IV. Tables 4.1 and 4.2
reveal that for a typical set of parameters such as radius of wire,
height of the wire above a ground plane, and length of the wire,
with the change in ground conductivity and dielectric constant,
there is not much change in the resonating natural frequencies
(zeros). But Tables 4.3 and 4.4 indicate that the real part of the
zeros becomes more negative with the decrement of the height of the
single wire above a ground plane. The agreement of this observa-
tion with the results obtained by other investigators verifies the
presented analysis of thin wire configurations.

44

It should also be noted that the crossed wire configuration illuminated by a plane wave does not excite all the natural modes. However, the crossed wire configuration excited from either end by a current source excitation does excite all the natural modes. The determined natural frequencies and the associated natural current modes thus obtained are in good agreement with those obtained by Crow, et al. [6] (as shown in Tables 4.5 and 4.6, and Figures 4.1 through 4.6).

REFERENCES

1. C. W. Oseen, "Über die elektromagnetische Schwingunden an dünnen Stäben," _Ark Mat. Astron. Fysik_, Vol. 9, No. 30, pp. 1-27, 1914.

2. E. Hállen, "Über die elecktrischen Schwingungen in drahtförmigen Leitern," _Uppsala Univ. Arssk._, No. 1, pp. 1-102,1930.

3. F. M. Tesche, "On the Singularity Expansion Method as Applied to Electromagnetic Scattering from Thin Wires," _Interaction Note 102, April 1972_; also _IEEE Trans. Ant. and Prop._, Vol. AP-21, 53 (1973).

4. D. R. Wilton, K. R. Umashanker, "Parametric Study of an L-shaped Wire Using the Singularity Expansion Method," _Interaction Note 152_, Nov. 1973.

5. T. H. Shumpert, "Currents Induced on Arbitrary Configurations of Wire Scatterers," (Ph. D.dissertation, Mississippi State University), May 1972.

6. T. T. Crow, C. D. Taylor and Murali Kumbale, "The Singularity Expansion Method Applied to Perpendicular Crossed Wires Over a Perfectly Conducting Ground Plane," submitted for publication in _IEEE Trans. on Antennas and Propagation_.

7. C. D. Taylor, R. S. Satterwhite, C. W. Harrison, Jr., "The Response of a Terminated Two-Wire Transmission Line Excited by a Nonuniform Electromagnetic Field," _IEEE Trans. on Ant. and Prop._, Vol. AP-13, No. 6, Nov. 1965 and also _Interaction Note 66_, Nov. 1965.

8. C. P. Bates, G. T. Hawley, "A Model for Currents and Voltages Induced Within Long Transmission Cables by an Electromagnetic Wave," _IEEE Trans. on Electromagnetic Compatibility_, Vol. EMC-13, No. 4, Nov. 1971.

9. L. Schlessinger, "Currents Induced by a Plane Wave on an Infinite Wire Above a Flat Earth," _IEEE Trans. on Electromagnetic Compatibility_, Vol. EMC-17, No. 3, Aug. 1974.

10. T. T. Crow, B. D. Graves, C. D. Taylor: "The Singularity Expansion Method as Applied to Perpendicular Crossed Cylinders in Free Space," _Interaction Note 161_, Oct. 1973.

11. T. T. Crow, B. D. Graves, C. D. Taylor, "Numerical Techniques Useful in the Singularity Expansion Method as Applied to Electromagnetic Interaction Problems," _Mathematics Note 27_, Dec. 1972.

12. R. W. P. King and T. T. Wu, "Analysis of Crossed Wires in a plane Wave Field," _IEEE Trans. on Elect. Comp._, Vol. EMC-17, Nov. 1975 and also _Interaction Note 216_, Jul. 1974.

13. E. D. Sunde, <u>Earth Conduction Effects in Transmission System</u>
    New York: Dover, 1969.

14. J. R. Wait, "Theory of Wave Propagation Along a Thin Wire
    Parallel to an Interface," <u>Radio Sci</u>., Vol. 7, June 1977.

15. C. E. Baum, "The Singularity Expansion Method," in <u>Transient
    Electromagnetic Fields</u>, L. B. Felsen (ed.), Springer-Verlag,
    Berlin, Heidelberg, New York, 1976.

16. K. R. Umashankar, T. H. Shumpert, and D. R. Wilton, "Scattering
    by Thin-Wire Parallel to a Ground Plane Using the Singularity
    Expansion Method," <u>IEEE Trans. Ant</u>. and <u>Prop</u>., Vol. AP-23, Mar.
    1975, and also "Transient Scattering by a Thin Wire in Free
    Space and Above Ground Plane Using the Singularity Expansion
    Method," <u>Interaction Note 236</u>, Aug. 1974.

17. L. Marin, "Natural Modes of Certain Thin-Wire Structures,"
    <u>Interaction Note 186</u>, August 1974.

18. C. D. Taylor, "External Interaction of the Nuclear EMP with
    Aircraft and Missile, <u>IEEE Trans. Ant</u>. and <u>Prop</u>., Vol. AP-26,
    Jan. 1978.

APPENDIX A

NATURAL MODES AND COUPLING COEFFICIENTS

The analytical expressions for the natural current modes for the associated first six natural frequencies as listed in Table 4.5 have been presented here:

For the $n = 1$ mode, $\omega_1 = 2.5680$ c/L, $L = 2\ell_\omega$.

$$I_a(z, j\omega_1) = 1.0 \quad \frac{\sin k_1 (\ell_a - z)}{\sin k_1 \ell_a} \quad \text{where} \quad k_1 = \frac{\omega_1}{c}$$

$$I_f(z', j\omega_1) = -0.15057 \quad \frac{\sin k_1(\ell_f - z')}{\sin k_1 \ell_f}$$

$$I_\omega(y', j\omega_1) = -0.42907 \quad \frac{\sin k_1(\ell_\omega - y')}{\sin k_1 \ell\omega}$$

For the $n = 2$ mode, $\omega_2 = 3.1416$ c/L

$$I_a(z, j\omega_2) = 0 \quad\quad\quad \text{where} \quad k_2 = \frac{\omega_2}{c}$$

$$I_f(z', j\omega_2) = 0$$

$$I'(y', j\omega_2) = \frac{\sin k_2(\ell_\omega - y')}{\sin k_2 \ell_\omega}$$

For the $n = 3$ mode, $\omega_3 = 4.0157$ c/L

$$I_a(z, j\omega_3) = -0.1114 \quad \frac{\sin k_3 (\ell_a - z)}{\sin k_3 \ell_a} \quad \text{where} \quad k_3 = \frac{\omega_3}{c}$$

$$I_f(z', j\omega_3) = 1.0 \quad \frac{\sin k_3(\ell_f - z')}{\sin k_3 \ell_f}$$

$$I_{\omega}(y', j\omega_3) \;=\; -0.44606 \; \frac{\sin k_3 (\ell_{\omega} - y)}{\sin k_3 \, \ell_{\omega}}$$

For the $n = 4$ mode, $\omega_4 = 6.2835 \; c/L$

$$I_a(z, j\omega_4) \;=\; 1.0 \; \frac{\sin k_4 (\ell_a - z)}{\sin k_4 \, \ell_a} \qquad\qquad \text{where} \quad k_4 = \frac{\omega_4}{c}$$

$$I_f(z', j\omega_4) \;=\; -0.998 \; \frac{\sin k_4 (\ell_f - z')}{\sin k_4 \, \ell_f}$$

$$I_{\omega}(y', j\omega_4) \;=\; -0.001 \; \frac{\sin k_4 (\ell_{\omega} - y')}{\sin k_4 \, \ell_{\omega}}$$

For the $n = 5$ mode, $\omega_5 = 7.9421 \; c/L$

$$I_a(z, j\omega_5) \;=\; 1.0 \; \frac{\sin k_5 (\ell_a - z)}{\sin k_5 \, \ell_a} \qquad\qquad \text{where} \quad k_5 = \frac{\omega_5}{c}$$

$$I_f(z', j\omega_5) \;=\; +0.275 \; \frac{\sin k_5 (\ell_f - z)}{\sin k_5 \, \ell_f}$$

$$I_{\omega}(y', j\omega_5) \;=\; -0.635 \; \frac{\sin k_5 (\ell_{\omega} - y')}{\sin k_5 \, \ell_{\omega}}$$

Lastly for the $n = 6$ mode, $\omega_6 = 9.4248 \; c/L$

$$I_a(z, j\omega_6) \;=\; 0 \qquad\qquad\qquad\qquad\qquad \text{where} \quad k_6 = \frac{\omega_6}{c}$$

$$I_f(z', j\omega_6) \;=\; 0$$

$$I_{\omega}(y', j\omega_6) \;=\; 1.0 \; \frac{\sin k_6 (\ell_{\omega} - y')}{\sin k_6 \, \ell_{\omega}}$$

49

The coupling coefficients for the first six natural modes are obtained as follows:

For $n = 1$ mode

$$-0.42907 \left(\frac{\eta_1}{c}\right) = \lim_{k \to k_1} j(k-k_1) \frac{-Z_f \tan \frac{k\ell_a}{2} + Z_a \tan \frac{k\ell_f}{2}}{k[Z_\omega(Z_a + Z_F) + 2 Z_a Z_f]}$$

Then at $k = k_1 + \frac{k}{100}$, where $k_1 = 2.568/L$, one obtains

$$\left(\frac{\eta_1}{c}\right) \simeq 0.0033$$

For $n = 2$ mode

$$1.0 \left(\frac{\eta_2}{c}\right) = \lim_{k \to k_2} j(k-k_2) \frac{-Z_f \tan \frac{k\ell_a}{2} + Z_z \tan \frac{k\ell_f}{2}}{k[Z_\omega(Z_a + Z_f) + 2 Z_a Z_f]}$$

Then at $k = k_2 + \frac{k_2}{100}$, where $k_2 = 3.1416/L$, one obtains

$$\left(\frac{\eta_2}{c}\right) \simeq 0.0$$

For $n = 3$ mode

$$-0.44606 \left(\frac{\eta_3}{c}\right) = \lim_{k \to k_3} j(k-k_3) \frac{-Z_f \tan \frac{k\ell_a}{2} + Z_a \tan \frac{k\ell_f}{2}}{k[Z_\omega(Z_a + Z_f) + 2 Z_a Z_f]}$$

Then at $k = k_3 + \frac{k_3}{100}$, where $k_3 = 4.0157/L$, one obtains

$$\left(\frac{\eta_3}{c}\right) \simeq 0.00296$$

For $n = 4$ mode

$$-0.001 \left(\frac{\eta_4}{c}\right) = \lim_{k \to k_4} j(k - k_4) \frac{-Z_f \tan\left(\frac{k\ell_a}{2}\right) + Z_a \tan\left(\frac{k\ell_f}{2}\right)}{k[Z_\omega(Z_a + Z_f) + 2 Z_a Z_f]}$$

Then at $k = k + \dfrac{k}{100}$, where $k = 6.284/L$, one obtains

$$\left|\frac{\eta_4}{c}\right| \simeq 0.0048$$

For $n = 5$ mode

$$-0.635 \left(\frac{\eta_5}{c}\right) = \lim_{k \to k_5} j(k - k_5) \frac{-Z_f \tan\left(\frac{k\ell_a}{2}\right) + Z_a \tan\left(\frac{k\ell_f}{2}\right)}{k[Z_\omega(Z_a + Z_f) + 2 Z_a Z_f]}$$

Then at $k = k_5 + \dfrac{k_5}{100}$, where $k_5 = 7.9421/L$, one obtains

$$\left(\frac{\eta_5}{c}\right) \simeq 0.00079$$

For $n = 6$ mode

$$1.0 \left(\frac{\eta_6}{c}\right) = \lim_{k \to k_6} j(k - k_6) \frac{-Z_f \tan\left(\frac{k\ell_a}{2}\right) + Z_a \tan\left(\frac{k\ell_f}{2}\right)}{k[Z(Z_a + Z_f) + 2Z_a Z_f]}$$

Then at $k = k_6 + \dfrac{\eta_6}{100}$, where $k_6 = 9.4248/L$, one obtains

$$\left(\frac{\eta_6}{c}\right) \simeq 0.0 \quad .$$

51